

Investigation of the Effect of Thermal Limiters on the Change in the Structure Formation of Deposited Multilayer Specimens from Steel AISI 308LSi

D.A. Chinakhov^{1,a}, K.O. Akimov^{2,3,b}, A.S. Dubrovskiy^{1,4,c}, E.D. Rzaev^{5,d}

¹Siberian State Industrial University, Novokuznetsk, 654007, Russian Federation

²Institute of Strength Physics and Materials Science SB RAS, Tomsk, 634055, Russian Federation

³National Research Tomsk State University, Tomsk, 634050, Russian Federation

⁴National Research Tomsk Polytechnic University, Tomsk, 634050, Russian Federation

⁵Azerbaijan Technical University, 25 G. Javid Avenue, AZ1148, Baku, Azerbaijan Republic

^achinakhov_da@mail.ru (corresponding author), ^bkibaarg@mail.ru,
^calexey.dubrovskiy.98@gmail.com, ^drasim-agma@rambler.ru

Keywords: additive manufacturing, thermal limiter, dendritic structure, hardness.

Abstract. The work investigated the effect of thermal limiters on the distribution of heat in the product and the formation of the structure of multilayer samples made of stainless steel AISI 308LSi deposited by electric arc welding in argon. It was found that as a result of the formation of products using thermal limiters, the high temperature regions deepen towards the substrate. It was revealed that the greatest effect of thermal limiters is observed in the central parts of the products. An increase in the fraction of γ -Fe is observed, which is confirmed by the dissolution of the dendritic axes of δ -Fe, in the sample obtained using thermal limiters. The obtained results confirm the prospects for producing multilayer products with increased mechanical properties by the method of electric arc welding using thermal limiters.

Introduction

The development of new technologies for the manufacture of parts of complex shapes with the required physical and mechanical properties is currently one of the priority tasks of modern production. The high rates of distribution and development of additive manufacturing technologies make it one of the most promising areas in solving the assigned tasks [1]. It is based on layer-by-layer metal deposition in accordance with a three-dimensional model created by means of computer-aided design [2, 3]. Automation and flexibility of production allowed to reduce the time and cost of development and implementation of complex geometric shapes of a large number of parts [4, 5]. International standard ISO / ASTM 52900 defines several types of additive manufacturing [6]. With regard to metal materials, the technologies of surfacing of powder materials [7-9] or wires [10-13] are distinguished. When using powder materials, difficulties arise associated with ensuring the consistency of the density and structure of the manufactured products [14-16]. In the case of differences in surface texture, sphericity of particles, chemical composition of the powder of one batch, an article with poor surface quality and a large number of pores may be formed.[17].

The technology of additive production of electric arc multilayer surfacing with a consumable electrode in a protective gas environment is one of the least expensive and has a high productivity. However, this process has its drawbacks, including significant residual stresses due to overheating [3, 5]. In the course of obtaining a product by layer-by-layer surfacing, an uneven distribution of heat occurs both in the volume of the workpiece and in the cross section. The use of thermal limiters in the form of forming graphite skids should contribute to the formation of the final picture of the temperature distribution in the product, i.e., the process of forming the structure must change.

The aim of this work is to study the effect of thermal limiters (forming graphite runners) on the change in the formation of the structure of multilayer samples made of AISI 308LSi stainless steel, obtained by layer-by-layer electric arc surfacing.

Materials and Methods

The heat distribution was simulated in the samples obtained by the method of layer-by-layer electric-arc growing: 1 - using thermal limiters (forming graphite skids); 2 - without thermal limiters. In fig. 1 shows three-dimensional models of samples obtained by the method of layer-by-layer electric arc surfacing.

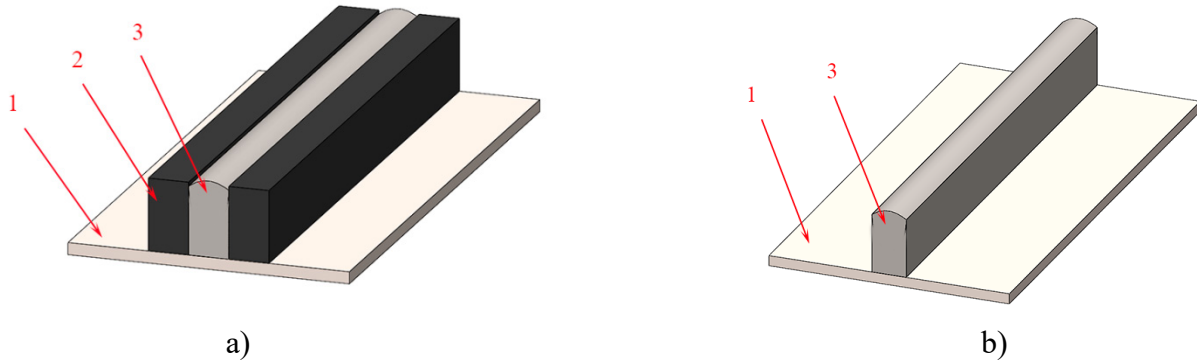


Fig. 1. Three-dimensional models of samples obtained by the method of layer-by-layer electric-arc surfacing: a) using thermal limiters (forming graphite skids), then sample No. 1; b) without the use of thermal limiters, then sample No. 2.

1 - stainless steel substrate, 2 - graphite forming skids (thermal limiters), 3 - sample.

The properties of the used material of steel AISI 308LSi are indicated in tab. 1 [18].

Table 1. Properties of AISI 308LSi steel.

Material	Thermal conductivity λ , W / mK	Elastic modulus E, GPa	Thermal-expansion coefficient α , K ⁻¹	Tensile strength σ_b , MPa	Melting temperature T_{melt} , °C
AISI 308LSi	12.642	193	$16.5 \cdot 10^{-6}$	590	1450

In fig. 2 shows the images of cross-sections of the samples with the designation of the boundary conditions and the direction of the input of the steel melting source. To simplify, the simulation was carried out in a two-dimensional plane of the cross section of the sample.

The following boundary conditions were applied: $T|_{L2}=1450^{\circ}\text{C}$, $u_x|_{L1}=0$, $u_x|_{L3}=0$, $u_y|_{L4}=0$.

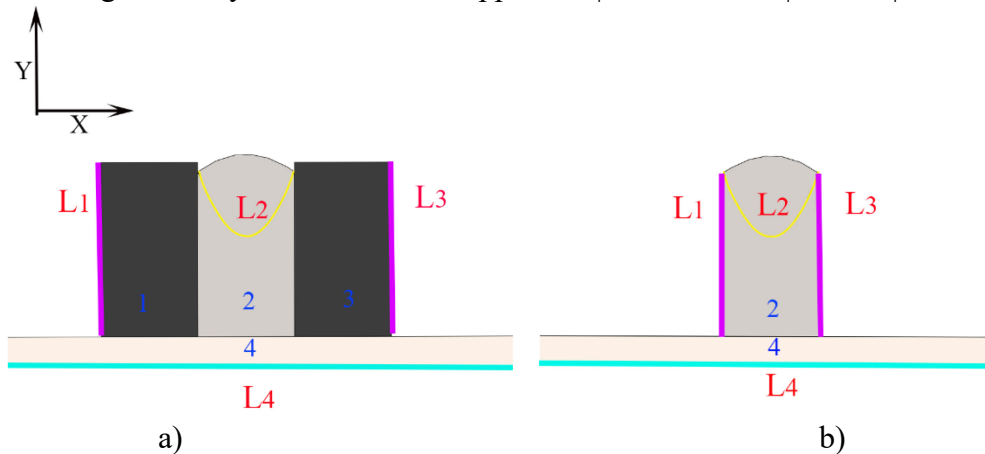


Fig. 2. Scheme of modeling of samples obtained by the method of layer-by-layer electric-arc surfacing, with boundary conditions: a) sample № 1; b) sample № 2.

1 and 3 - thermal limiters (forming graphite skids); 2 - sample; 4 - substrate.

The samples were obtained by multilayer arc welding with a consumable electrode AISI 308LSi 0.8 mm in diameter in argon, welding current $I_w = 100\text{A}$, arc voltage $U = 20\text{ V}$, gas consumption

$Q = 10$ l/min, reverse polarity. In fig. 3 shows photographs of layer-by-layer samples grown with AISI 308LSi welding wire in various external conditions.



a)

b)

Fig. 3. Photo of samples: a) sample № 1; b) sample № 2

Results and Discussion

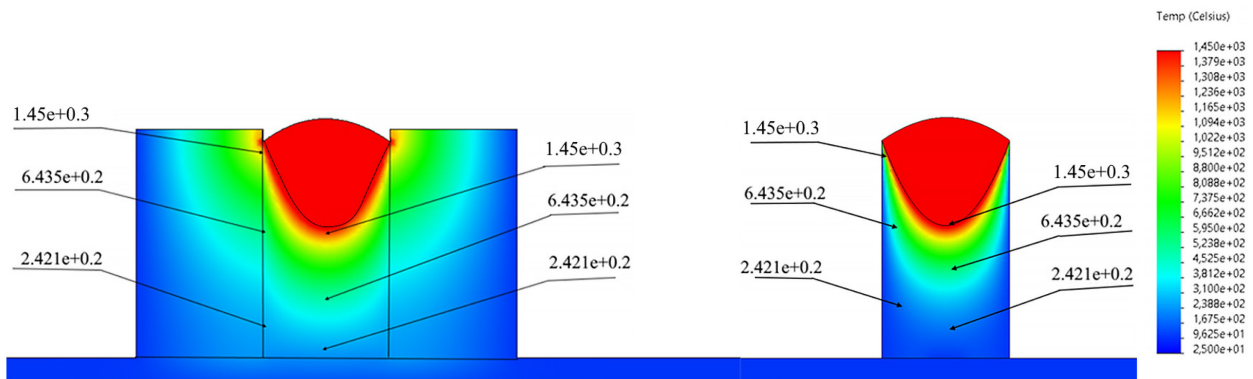


Fig. 4. Results of modeling the process of heating AISI 308LSi steel samples with a welding arc. Temperatures values are given in °C.

Analysis of the simulation results (Fig. 4) showed that when using thermal limiters, the maximum simulated temperature in sample 1 is 1474 °C (under specified conditions). In the case of surfacing sample 2 without using a thermal limiter, this value is 1450 °C. This difference is due to the presence of graphite skids providing a thermal barrier to the environment. For a better understanding of the processes occurring during layer-by-layer surfacing, it is necessary to consider the cooling curve of steel with a carbon content of up to 0.03% mass fraction (Fig. 5).

In this study, the temperature range of 911-1499 °C is of particular interest. In this temperature range an austenite phase is formed which has higher hardness values compared to the ferrite phase almost 2 times [19].

In fig. 6 shows the results of modeling the temperature distribution in the central and outermost lateral parts of the samples obtained under two different conditions. The shaded areas indicate areas that specify the fraction of the material located in the temperature range of the formation of the austenite phase.

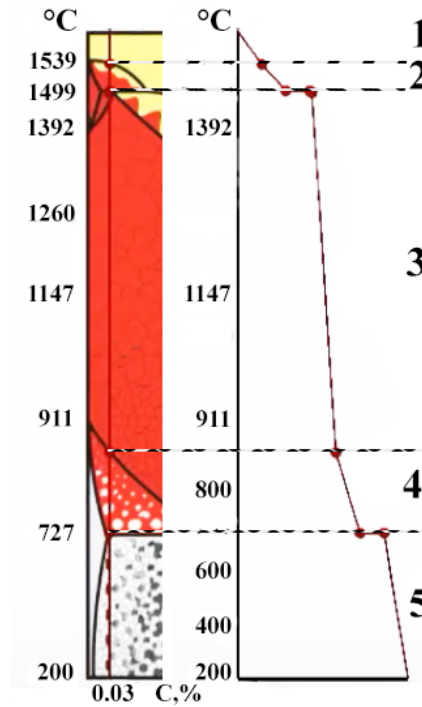


Fig 5. Cooling curve of steel with carbon content up to 0.03% mass fraction:
 1 - phase transformations do not occur, the liquid molten metal is cooled; 2 - crystallization of ferrite, the formation of δ -iron occurs, then in the region of 1494 ± 5 °C, the peritectic transformation δ -Fe + liquid phase \rightarrow γ -Fe occurs; 3 - the formation of the austenite phase occurs; 4 - below the temperature of 911 °C, the formation of the Austenite + β -Ferrite phase occurs; 5 - at temperatures below 727 °C, the α -Ferrite + III Cementite phase is formed.

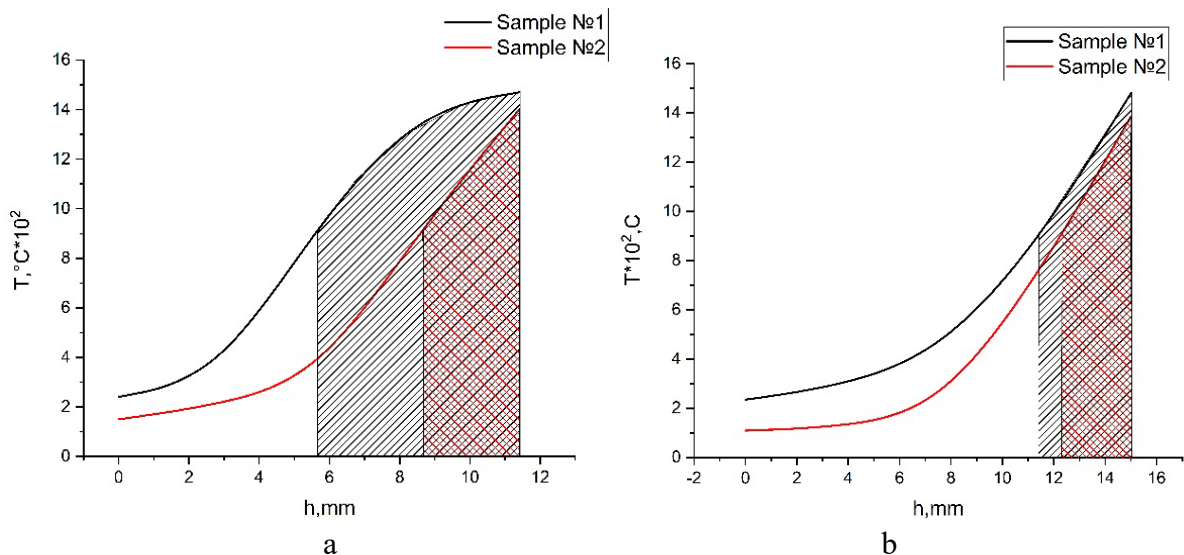


Fig. 6. Results of modeling the temperature distribution over the height of the samples: a) in the central part; b) in the outermost lateral part

Analysis of the simulation results in Fig. 6 showed that the use of forming graphite skids has the greatest effect on the temperature rise in the central part of the samples.

The proportion of metal in the central part of sample №1 located in the temperature range of the formation of the austenite phase is 2 times greater than in sample №2 obtained without using a heat limiter. In turn this ratio in the edge regions is 27% despite the use of thermal limiters in the form of graphite runners. It was found that when using graphite skids a greater temperature gradient arises between the edge and central parts of the sample, the difference in the proportion of metal in the

temperature range of austenite formation is 26% for sample 1 (50% of the metal in the central part, 23% of the metal in the edge). For sample №2, this difference is 7% (24% share in the central part, 17% share in the edge part). Thus, the use of thermal limiters in the form of graphite skids has a significant effect on the formation of the sample structure and leads to an increase in the fraction of the austenite phase by almost 2 times.

The curves describing heating in the region of the central layers (Fig. 6) were approximated by the least squares method. The resulting equation has the form $y = a + bx$, where b is the tangent of the angle of inclination, is also the first derivative of temperature with respect to time, which can be written as the rate of temperature change.

When obtaining sample № 1, the rate of temperature rise in the area of the central layers is $2.75 \cdot 10^2 \frac{^\circ\text{C}}{\text{s}}$, which is 33% more than that of sample №2, for which the rate of temperature rise was $1.85 \cdot 10^2 \frac{^\circ\text{C}}{\text{s}}$. For the edge lateral region of sample № 1, the rate of temperature rise in the area of the central layers is $0.78 \cdot 10^2 \frac{^\circ\text{C}}{\text{s}}$, and for specimen № 2, $0.74 \cdot 10^2 \frac{^\circ\text{C}}{\text{s}}$, i.e., 5% more. The temperature growth rate in the central part of sample № 1 is 72% higher than the temperature growth rate at the edge part, and for sample № 2 this ratio is 60%.

Also, in fig. 6 there are slight changes in the nature of the curve at a temperature of 911 °C for sample №1 and 340 °C for sample № 2. In the first case, after the inflection point (Fig. 6a), there is a decrease in the slope of the curve, or the heating rate. This is due to increased heat removal from the upper surface of the sample, since there is practically no heat removal from the lower surface due to the large volume of heated material in the central part. In the second case the change in the slope of the curve is associated with increased heat removal from all sides of the sample.

In what follows, we will consider the formation of the phase composition only in the central part of the samples. In fig. 7 shows curves characterizing the change in the width of dendrites along the height of the samples obtained under two different conditions.

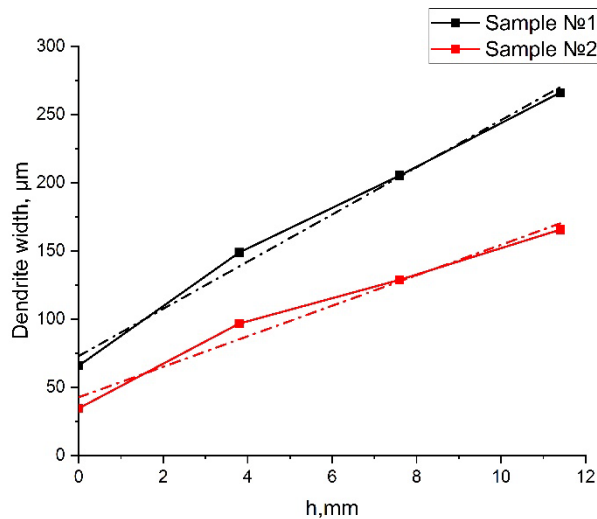


Fig. 7. Change in the width of dendrites along the height of the central part of the cross-section of the samples.

The use of thermal limiters (forming graphite skids) leads to enlargement of dendrites in the structure of the samples (Fig. 7) by an average of 200% in comparison with the sample obtained without using thermal limiters. The nature of the change in the curves in both cases is the same, without sharp bends. This indicates the uniformity of the effect of graphite skids on heating the sample. These data correlate well with the above simulation results. The obtained dependences were approximated by the least squares method. In sample №1, the dendrite enlargement rate is $17.3 \frac{\mu\text{m}}{\text{s}}$, which is 35% higher in the case of sample №2, for which the dendrite broadening rate is $11.18 \frac{\mu\text{m}}{\text{s}}$.

The dependences of the change in the width of the dendrites on temperature in the central part of the cross section of the samples (Fig. 8) were obtained on the basis of the data shown in Fig. 6 and 7.

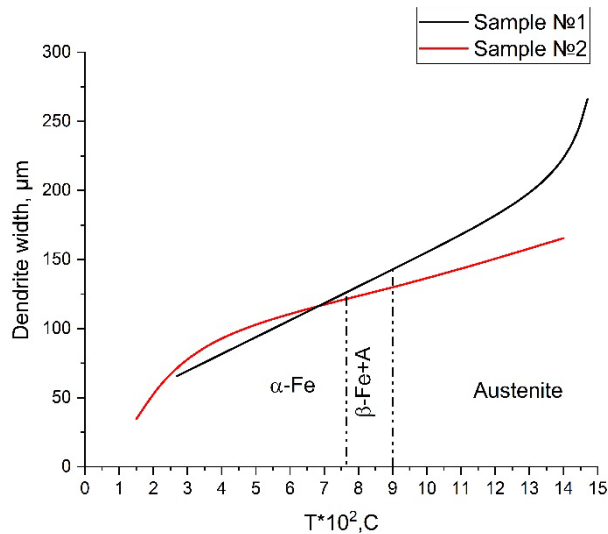


Fig. 8. Dependence of the width of dendrites on temperature in the central part of the cross section of the samples.

Analysis of the investigation results (Fig. 8) showed that most of the curve for sample No. 1 is located in the temperature range corresponding to the austenite phase. The obtained dependencies intersect in the region of 715 °C, close to the Kiryu Point, which can affect the magnetic properties of the products obtained [18]. A further increase in temperature (up to 1499 °C) leads to the formation of an austenite phase. The area of regions containing the austenite phase for samples №1 and №2 is 40% and 34%, respectively. Thus, it can be assumed that sample № 1 will have a smaller amount of δ -Fe phase than sample №2. Qualitative analysis of the optical images of the structures of the samples was carried out to confirm this. In fig. 10 (a-f) shows optical images of the structures of the central parts of the billets in layers, obtained in two different conditions.

In fig. 10 (b, d, f) it can be seen that the growth of long colonies of δ -ferrite prevails in sample № 2. The primary order axes of these dendrites are oriented along the sample height. Changes in the morphology of δ -ferrite in sample No. 1 are clearly visible in Fig. 10 (a, c, e). Ferritic branches are broken and partially dissolved in these samples. The most pronounced dissolution and fragmentation of dendritic axes is observed in the middle part of the sample. In the process of crystallization of molten metal, the process of polymorphic transformation δ -Fe \rightarrow γ -Fe begins. Due to the fact that the metal of sample № 1 is at temperatures higher than the metal of sample № 2, then the process of diffusion of δ -ferrite into austenite takes place in it. Similar changes in the phase composition were established in [20], where the authors subjected the samples obtained by electron-beam surfacing from AISI 304 steel, followed by heat treatment followed by quenching in water.

Conclusion

According to the research results, it was found that the use of thermal limiters (forming graphite skids) has a positive effect on the formation of an equilibrium phase structure in samples obtained by the method of layer-by-layer electric arc surfacing. The greatest influence of thermal limiters on the structure of AISI 308LSi steel is observed in the central parts of the samples obtained. In turn, the process of dendrite enlargement is observed. It was revealed that the use of thermal limiters allows you to increase the proportion of γ -Fe in the volume of products obtained. An active process of diffusion of δ -ferrite into austenite in specimens obtained with thermal restraints (graphite skids) has been established, which, presumably, will improve the mechanical properties of the entire product.

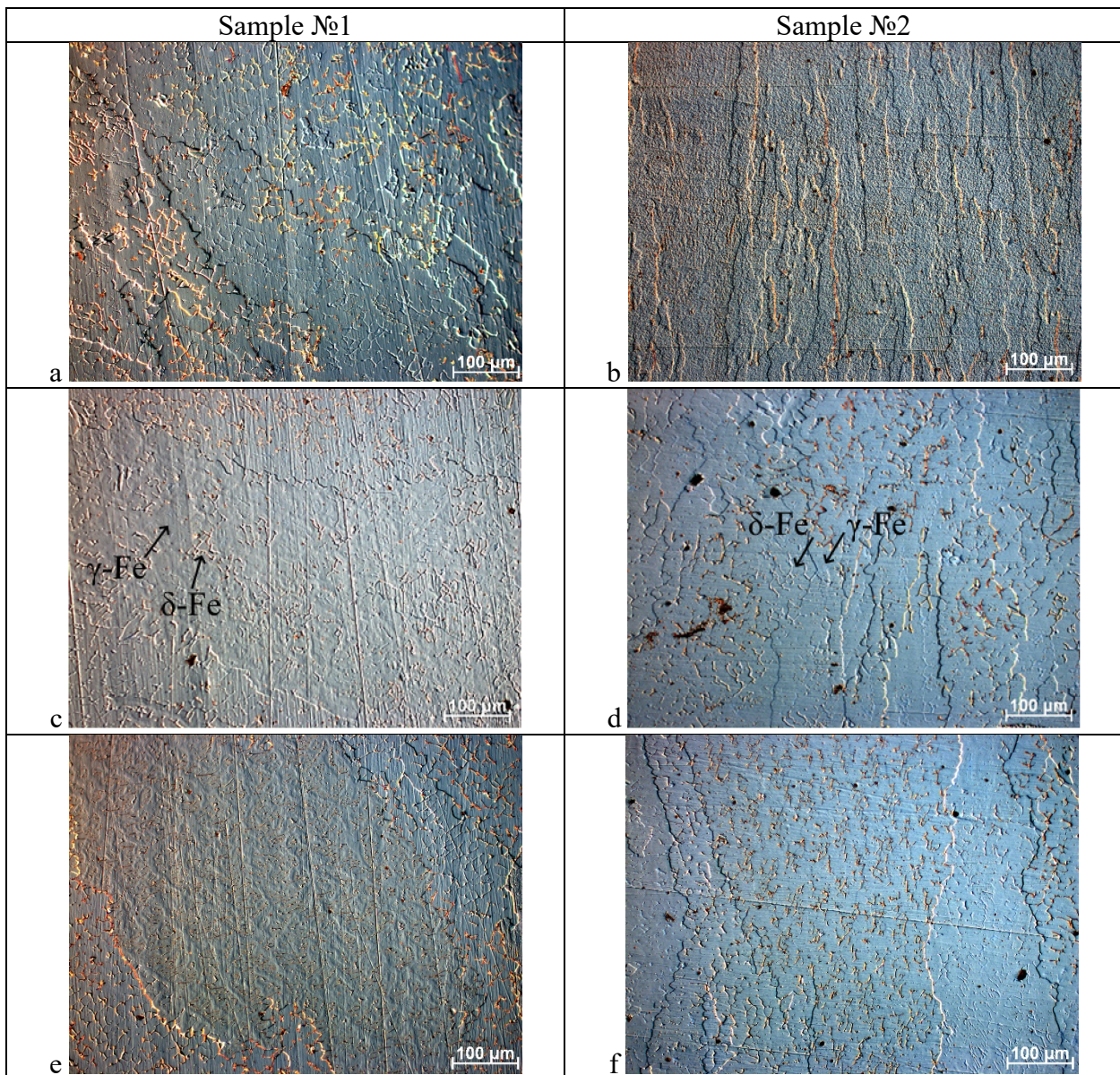


Fig. 10. Optical images of the structures of the central parts of the samples by layers:
a, b - first layer; c, d - second layer; e, f - third layer.

References

- [1] Wohlers T., Wohlers report 2014: Additive manufacturing and 3D-printing state of the industry: Annual worldwide progress report, Wohlers Associates, 276 p.
- [2] ASTM F2792-12a Standard terminology for additive manufacturing technologies
- [3] Kuznetsov M.A., Danilov V.I., Krampit M.A., Chinakhov D.A., Slobodyan M.S. Mechanical and tribological properties of a metal wall grown by an electric arc method in an atmosphere of shielding gas. *Obrabotka metallov (tekhnologiya, oborudovanie, instrumenty) = Metal Working and Material Science*, 2020, vol. 22, no. 3, pp. 18–32. DOI: 10.17212/1994-6309-2020-22.3-18-32. (In Russian).
- [4] X. Yan, P. Gu, A review of rapid prototyping technologies and systems, *Comput. Aided Des.* 28 (4) (1996) 307–318, [https://doi.org/10.1016/0010-4485\(95\)00035-6](https://doi.org/10.1016/0010-4485(95)00035-6).
- [5] Gisario A., Kazarian M., Martina F., Mehrpouya M. Metal additive manufacturing in the commercial aviation industry: a review. *Journal of Manufacturing Systems*, 2019, vol. 53, pp. 124–149. doi: 10.1016/j.jmsy.2019.08.005

-
- [6] DIN EN ISO/ASTM 52900:2018–06, Additive Manufacturing; Deutsche und Englische Fassung prEN_ISO/ASTM 52900:2018.
- [7] Murr L.E., Gaytan S.M., Ramirez D.A., Martine, E., Hernandez J., Amato K.N., Shindo P.W., Medina F.R., Wicker R.B. Metal fabrication by additive manufacturing using laser and electron beam melting technologies. *Journal of Materials Science and Technology*, 2012, vol. 28, iss. 1, pp. 1–14. doi: 10.1016/S1005-0302(12)60016-4
- [8] Gu D.D., Meiners W., Wissenbach K., Poprawe R. Laser additive manufacturing of metallic components: materials, processes and mechanisms. *International Materials Reviews*, 2012, vol. 57, iss. 3, pp. 133–164. doi: 10.1179/1743280411Y.0000000014
- [9] Sing S.L., An J., Yeong W.Y., Wiria F.E. Laser and electron-beam powder-bed additive manufacturing of metallic implants: A review on processes, materials and designs. *Journal of Orthopaedic Research*, 2016, vol. 34, iss. 3, pp. 369–385. doi: 10.1002/jor.23075
- [10] Queguineur A., Rückert G., Cortial F., Hascoët J.Y. Evaluation of wire arc additive manufacturing for large-sized components in naval applications. *Welding in the World*, 2018, vol. 62, iss. 2, pp. 259–266. doi: 10.1007/s40194-017-0536-8
- [11] Rodriguez N., Vázquez L., Huarte I., Arruti E., Taberero I., Alvarez P. Wire and arc additive manufacturing: a comparison between CMT and Top TIG processes applied to stainless steel. *Welding in the World*, 2018, vol. 62, pp. 1083–1096. doi: 10.1007/s40194-018-0606-6
- [12] Chinakhov D.A., Akimov K.O., Dubrovskiy A.S., Ilyaschenko D.P. Influence of Thermal Limiters on the Formation of the Dendritic Structure of the Welded Stainless Steel Layer. *Journal of Physics: Conference Series* 1945 (2021) 012038. doi:10.1088/1742-6596/1945/1/012038
- [13] Bekker A. C. M., Verlinden J. C. Life cycle assessment of wire + arc additive manufacturing compared to green sand casting and CNC milling in stainless steel. *Journal of Cleaner Production*, 2018, vol. 177, pp. 438–447. doi: 10.1016/j.jclepro.2017.12.148
- [14] Murr L.E., Martinez E., Amato K.N., Gaytan S.M., Hernandez J., Ramirez D.A., et al. Fabrication of metal and alloy components by additive manufacturing: examples of 3d materials science. *J Mater Res Technol* 2012; 1:42–54. [https://doi.org/10.1016/s2238-7854\(12\)70009-1](https://doi.org/10.1016/s2238-7854(12)70009-1)
- [15] James W.J., List F.A., Pannala S., Dehoff R.R., Babu S.S. The metallurgy and processingscience of metal additive manufacturing. *Int Mater Rev* 2016; 61:315–60. <https://doi.org/10.1080/09506608.2015.1116649>
- [16] Slotwinski J.A., Garboczi E.J., Stutzman P.E., Ferraris C.F., Watson S.S., Peltz M.A. Characterization of metal powders used for additive manufacturing. *J Res Natl InstStand Technol* 2014; 119:460. <https://doi.org/10.6028/jres.119.018>
- [17] Strondl A., Lyckfeldt O., Brodin H., Ackelid U. Characterization and control of powder properties for additive manufacturing. *JOM* 2015; 67:549–54. <https://doi.org/10.1007/s11837-015-1304-0>.
- [18] Steel symbol/number: X2CrNi21–10/1.4331 [electronic resource]. Access mode: www.url:https://materials.springer.com/lb/docs/sm_lbs_978-3-540-44760-3_97. 09.07.2021.
- [19] *Metallurgie und Werkstofftechnik: e. Wissensspeicher. 2 Bände R. Zimmermann, K. Günther. 1977.*
- [20] E.G. Astafurova, M.Y. Panchenko, V.A. Moskvina, G.G. Maier, S.V. Astafurov, E. V. Melnikov, A.S. Fortuna, K.A. Reunova, V.E. Rubtsov, E.A. Kolubaev, Microstructure and grain growth inhomogeneity in austenitic steel produced by wire-feed electron beam melting: the effect of post-building solid-solution treatment, *J. Mater. Sci.* 55 (2020) 9211–9224, <https://doi.org/10.1007/s10853-020-04424-w>